EBioMedicine 50 (2019) 55–66

Contents lists available at ScienceDirect

EBioMedicine

journal homepage: www.elsevier.com/locate/ebiom

Research paper

Aberrant expression of embryonic mesendoderm factor MESP1 promotes tumorigenesis

Neha Tandon[a], Kristina Goller[a], Fan Wang[a,b], Benjamin Soibam[c], Mihai Gagea[d], Abhinav K. Jain[e], Robert J. Schwartz[a], Yu Liu[a,*]

[a] Department of Biology and Biochemistry, University of Houston, Houston, TX, United States
[b] Department of Oncology, the First Affiliated Hospital of Xi'an Jiaotong University, Xi'an, Shaanxi Province, China
[c] Computer Science and Engineering Technology, University of Houston-Downtown, Houston, TX, United States
[d] Department of Veterinary Medicine and Surgery, The University of Texas MD Anderson Cancer Center, Houston, TX, United States
[e] Center for Cancer Epigenetics, Department of Epigenetics and Molecular Carcinogenesis, The University of Texas MD Anderson Cancer Center, Houston, TX, United States

ARTICLE INFO

Article History:
Received 15 April 2019
Revised 7 November 2019
Accepted 7 November 2019
Available online 21 November 2019

Keywords:
Mesp1
ARF
Lung cancer
Lineage-survival oncogene

ABSTRACT

Background: Mesoderm Posterior 1 (MESP1) belongs to the family of basic helix-loop-helix transcription factors. It is a master regulator of mesendoderm development, leading to formation of organs such as heart and lung. However, its role in adult pathophysiology remains unknown. Here, we report for the first time a previously-unknown association of MESP1 with non-small cell lung cancer (NSCLC).
Methods: MESP1 mRNA and protein levels were measured in NSCLC-derived cells by qPCR and immunoblotting respectively. Colony formation assay, colorimetric cell proliferation assay and soft agar colony formation assays were used to assess the effects of MESP1 knockdown and overexpression in vitro. RNA-sequencing and chromatin immunoprecipitation (ChIP)-qPCR were used to determine direct target genes of MESP1. Subcutaneous injection of MESP1-depleted NSCLC cells in immuno-compromised mice was done to study the effects of MESP1 mediated tumor formation in vivo.
Findings: We found that MESP1 expression correlates with poor prognosis in NSCLC patients, and is critical for proliferation and survival of NSCLC-derived cells, thus implicating MESP1 as a lung cancer oncogene. Ectopic MESP1 expression cooperates with loss of tumor suppressor ARF to transform murine fibroblasts. Xenografts from MESP1-depleted cells showed decreased tumor growth in vivo. Global transcriptome analysis revealed a MESP1 DNA-binding-dependent gene signature associated with various hallmarks of cancer, suggesting that transcription activity of MESP1 is most likely responsible for its oncogenic abilities.
Interpretation: Our study demonstrates MESP1 as a previously-unknown lineage-survival oncogene in NSCLC which may serve as a potential prognostic marker and therapeutic target for lung cancer in the future.

Research in context

Evidence before this study

Lung cancer is the leading cause of cancer-related deaths in the United States. Many driver oncogenes responsible for the disease have been reported previously. Adding to this growing list are 'lineage-survival oncogenes', master transcription factors of a cell lineage that are essential for the survival of cancers derived from that lineage. Transcription factor MESP1 is the earliest marker of nascent mesoderm during embryonic development, resulting in the formation of all cardiac cell types. In addition, MESP1 also plays important roles in the formation of organs of endodermal origin, such as lung. However, expression profile and functions of MESP1 in adult pathophysiology, including human cancer remains unknown.

Added value of this study

In this study, we demonstrated that MESP1 is aberrantly expressed in cells and tissues of lung cancer, and NSCLC-derived cells depend on MESP1 for proliferation, colony formation and subcutaneous tumor formation in immuno-compromised mice. Our genome-wide transcriptome analyses using various cellular systems is the first to uncover transcriptional activity of MESP1 in lung cancer. Mechanistically, we found MESP1 is enriched at the chromatin and induce expression of several target genes that have defined functions in various

* Corresponding author.
E-mail address: yliu54@uh.edu (Y. Liu).

https://doi.org/10.1016/j.ebiom.2019.11.012

hallmarks of cancer. Co-expression of MESP1 and its target genes predicted poor prognosis in lung cancer patients.

Implications of all the available evidence

Our work provides the first evidence of aberrant expression, functional relevance and transcriptome-profiles of MESP1, which may serve as a promising biomarker and a therapeutic target in lung cancer.

1. Introduction

Lung cancer causes the most cancer-related deaths in both men and women in the United States and worldwide [1,2]. About 15% of lung cancers are categorized as small cell lung cancer and rest as NSCLC. Two major subtypes of NSCLC, adenocarcinoma (~50%) and squamous cell carcinoma (~40%) are defined based on histopathological features [3]. At advanced stage of the disease, 5-year survival rate for lung cancer (4.7%) is lower than other leading cancers, such as breast cancer (27%), prostate cancer (30%), colorectal cancer (13.8%) and melanoma of skin (22.5%) [4]. Multi-disciplinary efforts of the past decade have improved our understanding of the molecular pathogenesis of this disease. Key molecular alterations found in lung cancer span various gene families, such as receptor tyrosine kinases (*EGFR, ALK, HER2, FGFR2*), signaling (*KRAS, NF1*), epigenetic factors (*EZH2*), transcription factors (*MYC*), cell cycle (*CDKN2A*) and tumor suppressors (*TP53, PTEN*)[3]. However, given the dismal survival rates, there remains an unmet medical need for identification of additional oncogenic drivers and predictive biomarkers to allow for more precise prognosis and treatment for the patients.

During development, certain master regulatory genes play key roles in cell specific lineage determination by controlling various growth-promoting signaling mechanisms. The emerging theory of lineage addiction model proposes that altering the expression of these lineage-survival genes can give rise to precancerous cells with survival advantage and inbuilt framework to progress to full tumorigenicity [5]. For example, *MITF*, a master regulator of melanocyte development, is a melanoma oncogene [6], *SOX2*, a pluripotency-specific transcription factor, is required for lung and esophageal squamous cell carcinoma [7], and thyroid transcription factor *TITF1/NKX2.1* is involved in lung adenocarcinoma [8].

Mesoderm Posterior 1 (MESP1) is a basic helix-loop-helix transcription factor transiently expressed in nascent mesoderm of mice at E6.5 - E7.0. It is widely known as a master regulator of cardiovascular lineage in normal development [9]. Functionally, MESP1 binds to canonical E-box motif (CACGTG) [10] to trigger the expression of a cascade of lineage-specific transcription factors. MESP1 null mouse embryos develop cardiac malformation, leading to embryonic lethality at E10.5 [11]. MESP1, in combination with ETS2 is sufficient to transdifferentiate human dermal fibroblasts into cardiac progenitors [12]. In a context-dependent manner, MESP1 can also regulate hematopoietic and skeletal myogenic differentiation [13]. Recently, MESP1 knockdown has been shown to attenuate vascular lineage differentiation of human induced pluripotent stem cells (iPSCs) [14]. MESP1 is exclusively required for Epithelial to Mesenchymal transition (EMT) in cardiovascular progenitors and its knockdown decreased expression of EMT transcription factors *SNAI1* and *TWIST1* in vascular progenitors [14–16] Agreeing with the involvement of Mesp1 in broad lineages, our previous work demonstrated that Mesp1 directly targets genes essential for mesendoderm formation, which further develops into organs such as heart, lung, liver and kidney, to name a few [10]. Despite being a critical factor in embryogenesis, Mesp1's expression and function in postnatal pathophysiological processes is unknown.

Analysis of TCGA data revealed that elevated MESP1 expression is associated with a range of cancers, primarily in organs of mesendoderm origin, thus, putting forth MESP1 as a potential lineage-survival oncogene that remains unexplored in lung cancer or any other cancer-type. In this study, we report that MESP1 knockdown in NSCLC cells attenuated cell proliferation and survival. MESP1 overexpression induced cellular proliferation and transformation, an effect found to be dependent on DNA-binding ability of MESP1. Global transcriptome analyses (RNA-Seq) followed by Chromatin Immunoprecipitation (ChIP) revealed that MESP1 directly regulates various genes involved in multiple hallmarks of cancer. High MESP1 expression and a gene signature regulated by MESP1 correlates with poor prognosis in NSCLC patients. To our knowledge, this is the first report of MESP1 as regulator of oncogenesis.

2. Materials and methods

2.1. Plasmids and site-directed mutagenesis

Mouse Mesp1 cDNA was obtained from in-house RNA library and was cloned into pENTR1a using Gateway technology. After sequence verification, Mesp1-pENTR1a was then transferred into tet-inducible expression vector - pLIX403 (Addgene # 41395) using LR Reaction. Lentiviral vector containing open-reading frame for MESP1 with C-Avi-FLAG tag was purchased from GeneCopoeia (V0883-Lv242). For generating EK-mutant of mouse Mesp1 and human MESP1, site-directed mutagenesis kit from Millipore (KOD Xtreme Hot start DNA polymerase Cat # 71975) was used. The PCR primers used for mutagenesis are included in the Supplementary Table T1. shRNA mediated knockdown of hMESP1 was done using shRNA lentiviral (pLKO.1-puro) plasmids from Dharmacon (Clone ID: TRCN0000107835 and TRCN0000107836).

2.2. Cell lines, cell culture and transfection

Human lung cancer cell lines (H358, A549, H1944, H1299 and H460) and BEAS-2B from ATCC were cultured according to the supplier's protocol. $p19^{ARF}$ null MEFs and *p53* null MEFs were kind gifts from Dr. Martine F. Roussel and Dr. Charles J. Sherr (St. Jude Children's Research Hospital) and Dr. Michelle C. Barton (The University of Texas MD Anderson Cancer Center) respectively. Both MEFs were grown in DMEM media (Thermo Scientific) with 10% FBS, with extra additives for $p19^{ARF}$ null MEFs (MEM non-essential amino acids, β-mercaptoethanol and gentamycin). $p19^{ARF}$ null MEFs were grown in a 9% CO_2 incubator. MESP1-knockdown and Mesp1-overexpressing stable cell lines were generated using lentiviruses as described in previously published protocol [17]. In order to establish doxycycline-inducible Mesp1-V5 expression system, cells were incubated with 1 μg/ml of doxycycline (Sigma) for 15–20 days with fresh doxycycline being replenished every 48 h.

2.3. Cell proliferation, colony formation and soft agar colony formation assays

To study cell proliferation, cells were seeded in 96-well plates at 1000 cells/well in respective medium and counted every 48 h for up to 6 days, using MTS assay as per manufacturer's (Promega) instructions. Cells were replenished with fresh media (for cancer cell lines) and doxycycline-containing media (for MEFs) every 48 h. In order to perform colony formation assay in lung cancer cell lines, 1000 cells were seeded in 6-well plate and incubated for 10 days after which they were fixed and stained with 0.1% crystal violet prepared in 100% methanol. In order to perform colony formation assay in MEFs, 10,000 cells were seeded in 10 cm dishes and incubated for 14 days after which they were fixed and stained with 0.1% crystal violet prepared in 100% methanol. For soft agar colony formation assays, 300,000 MEFs were seeded in 4 ml of DMEM culture medium with 0.35% low-melting-temperature agarose (BD Biosciences) overlaying

1.5 mL of 0.7% low-melting agarose in 6-well plates and incubated at 37 °C for 1 month [18]. Soft agar was overlaid with fresh 400 μl of doxycycline-containing media every 48 h, so that final concentration of doxycycline in each well was 1 μg/ml. All experiments were done in triplicates except for cell proliferation for which four replicates were set up for each cell type. Soft agar images were taken using Leica Stereo-microscope and Nikon microscope.

2.4. Patient RNA samples

Normal lung, squamous cell lung carcinoma and lung adenocarcinoma patient RNA samples were purchased from OriGene Technologies. List of patient samples is in Supplementary Table T2.

2.5. RNA isolation and quantitative real-time PCR (qRT-PCR)

Total RNA was isolated using TRIzol reagent (Invitrogen) according to the manufacturer's protocol. First strand cDNA synthesis and qRT-PCR was performed using Takyon One-Step kit converter – Euroscript II and Takyon Rox SYBR MasterMix dTTP Blue (Eurogentec). Real-time quantitative PCR was performed (Applied Biosystems 7500) using the cycling conditions: 48 °C for 10 min (reverse transcription); 95 °C for 3 min (Initial denaturation); 40 cycles of 95 °C for 10 secs, 60 °C for 30 secs, 72 °C for 30 secs. All qRT-PCRs were set up in duplicates using three biological replicates for each sample. The PCR primers used for qRT-PCR are included in Supplementary Table T1.

2.6. Chromatin immunoprecipitation (ChIP) assay

Cells were grown in 10 cm culture dishes to 75%–80% confluency. Cells were fixed with 1% formaldehyde in culture medium. The fixation reaction was stopped by addition of glycine. Cells were collected in ice cold PBS containing protease inhibitors and PMSF. Each ChIP cell pellet was made from two 10 cm dishes. The ChIP pellets were processed further using the ChIP-IT Express kit according to manufacturer's instructions (Active Motif, Cat# 53008). After the ChIP DNA was obtained, PCR was performed using primers (Supplementary Table T1) to amplify genomic regions containing E-box binding motifs. Enrichment for each gene locus was calculated as fold enrichment for hMESP1 antibody relative to control IgG antibody.

2.7. Western blot and antibodies

Whole cell lysates were isolated in RIPA buffer, followed by estimation of protein concentration by Pierce BCA protein assay kit (Thermo Scientific). Protein samples were gel electrophoresed on 4%–12% Bis-Tris gels (Thermo Scientific), followed by transfer to polyvinylidene difluoride membrane. The membrane was blocked in 5% milk/PBST buffer, then incubated overnight with primary antibodies at 4 °C. After being incubated with the respective secondary antibody, blots were developed using film radiography. Antibodies used were: anti-MESP1 (ab173011 and ab230308); anti-FLAG (Cell Signaling, 8146S); anti-CDKN2A/p19ARF (ab80); anti-p14 ARF (Cell Signaling, 2407S); anti-V5 tag (MCA1360GA Biorad); anti-beta actin (AM1021b); anti-normal mouse IgG (Millipore-sigma 12-371); anti-p53 (sc-126 and sc-98).

2.8. Immunohistochemistry and analyses

Immunohistochemistry (IHC) of lung cancer and prostate tumor arrays (LC2084, MNT241a, and BCN601, US Biomax) was performed using a VECTASTAIN Elite ABC kit and a DAB Detection kit (Vector Laboratories) with an anti-MESP1 antibody (1:750 dilution; ab230308, Abcam). Briefly, tumor arrays were de-paraffinized in xylene, followed by rehydration in ethanol. Antigen retrieval was done in sodium citrate buffer (pH 6) in a microwave at 199°F, following which endogenous peroxidase activity was blocked using 0.3% hydrogen peroxide in water. Non-specific binding was blocked using normal goat serum (Vectastain ABC kit). Arrays were then incubated in primary antibody overnight at 4 °C. Next day, after incubation in biotinylated secondary antibody (Vectastain ABC kit), arrays were developed. Tumor arrays were counterstained using Gills formula Haematoxylin (Vector laboratories), dehydrated in ethanol, incubated in xylene and then mounted with Glycergel mounting media. Images at 5X objective magnification were taken with Aperio scanner and Image Scope software and at 40X objective magnification using Olympus BX41 microscope and Leica DFC495 microscope camera. The IHC staining was evaluated by applying a scoring system from 0 to 3 (0=negative or no staining, 1 = weak or low staining; 2 = moderate or intermediate staining; and 3 = strong or high staining). The score for each tissue was determined based on the percentage of positive cells and intensity of staining. The slides were read by a pathologist using Olympus BX41 microscope.

2.9. GSEA analysis of differentially expressed genes

Gene set enrichment analysis (GSEA) was performed using the Molecular Signature Database (MSigDB v6.2) online version [19]. All significantly expressed genes were ranked by adjusted Log2 fold change and tested against H: Hallmark gene sets to look for enrichment.

2.10. Data mining

In order to determine MESP1 expression in various cancers, publicly available TCGA and GTEx datasets from cBioportal and GEPIA [20] were used. The Kaplan–Meier (KM) plot for survival curve analysis was performed using TCGA and GTEx datasets from GEPIA[20]; the cut-off used was 30th percentile of MESP1 expression.

2.11. Animal studies and imaging

Subcutaneous injections were done in the right flank of 6–8 week immunodeficient NOD-SCID-Gamma mice (NSG) (Jackson Laboratories). 2.5×10^6 cells in 200 μl of PBS were injected for both H358 and A549 cell lines. For H358, 5 mice each were injected for both control and knockdown cell lines whereas for A549, 6 mice were used for each group. Tumor size was monitored twice weekly using calipers and tumor volume was calculated using the formula: Tumor volume $(mm^3) = [\text{length (mm)} \times \text{width (mm)}^2] \times 0.5$. For H358, tumors were harvested 15 days post-injection, while for A549, tumors were harvested 38 days post-injection. Following harvesting, weights of individual tumors were measured. Sections from formalin-fixed paraffin embedded tumor tissues were used for hematoxylin & eosin (H&E) staining. Slides were read using Olympus BX41 microscope by a pathologist. The animal studies were approved by Institutional Animal Care and Use Committee (IACUC) at University of Houston.

3. Results

3.1. Expression of MESP1 is elevated in lung cancer patients

To determine if MESP1 is involved in human cancers, we first analyzed the expression of MESP1 in various cancer types using the global gene expression data available through TCGA [20–22]. Interestingly, MESP1 expression is upregulated in various cancers with the most common type of NSCLC, lung adenocarcinoma, among the top hits (Supplementary Fig. S1a). To further validate these findings, the relative expression of the *MESP1* transcript was examined in various cancer types with respect to their

normal corresponding tissue using TCGA and GTEx datasets. *MESP1* expression was elevated in a number of cancers (Fig. 1a), including lung adenocarcinoma (LUAD) ($n = 483$) and squamous cell carcinoma (LUSC) ($n = 486$), which showed significantly higher *MESP1* expression levels with respect to normal lung tissue (Fig. 1b). Slightly higher level was visible in LUAD patients than LUSC patients. Additionally, MESP1 expression was consistently upregulated across all stages of lung cancer, suggesting the importance of this gene throughout disease progression (Fig. 1b).

Next, we validated the aberrant expression of *MESP1* by qRT-PCR analysis of patient RNA samples of lung squamous cell carcinoma ($n = 5$), lung adenocarcinoma ($n = 5$) and normal lung tissue ($n = 5$) (Fig. 1c). Compared to the normal lung tissues, *MESP1* expression was significantly higher in lung adenocarcinoma patient samples as well as in lung squamous cell carcinoma patient samples (Fig. 1c). The level of change in *MESP1* expression in patient derived RNA samples is consistent with the expression changes observed in TCGA and GTEx datasets (Fig. 1b). We also analyzed MESP1 expression in various lung cancer cell lines and a nonmalignant bronchial epithelial cell line BEAS-2B. MESP1 expression (RNA and protein) was significantly higher in all cancer cell lines representing NSCLC than nonmalignant BEAS-2B (Fig. 1d).

The deregulation of MESP1 was further analyzed by immunohistochemistry (IHC). IHC staining was performed on human tissue microarrays (LC2084, MNT241A, and BCN601, US Biomax) consisting of samples of normal lung tissues ($n = 14$), normal adjacent tumor tissues ($n = 10$), lung adenocarcinoma ($n = 74$), and lung squamous cell carcinoma tissues ($n = 108$). While majority of normal lung tissue and normal adjacent tissue stained negative (Score = 0) and low (Score = 1) for MESP1 expression, most lung adenocarcinoma and squamous cell carcinoma samples showed intermediate and high (Score = 2 and 3, respectively) level of MESP1 protein (Fig. 1e). Intermediate and high MESP1 levels were associated with all stages of adenocarcinoma and squamous cell carcinoma (Supplementary Fig. S1b), suggesting that MESP1 may be essential for maintaining malignant phenotypes. Additionally, MESP1 IHC in prostate specimens (BCN601 and MNT241A, US Biomax) revealed higher expression of MESP1 in tumor samples ($n = 9$) than corresponding normal tissues ($n = 4$) (Supplementary Fig. S1c). We chose prostate cancer for IHC analyses because prostate cancer shows the highest expression of MESP1 in the TCGA datasets (Supplementary Fig. S1a). For detailed histopathology report, see Supplementary Table T3.

3.2. MESP1 regulates growth and cell proliferation of NSCLC cells

To determine if MESP1 is required for NSCLC cell growth, A549 and H358 NSCLC-derived cells were transduced independently with two shRNAs that target *MESP1*. In comparison to scrambled shRNA (shcontrol), the expression of MESP1 (protein and RNA) was significantly downregulated by both shRNAs with varying efficiency (Fig. 2a). We performed MTS assay to determine the effects of MESP1 on cell proliferation and observed that MESP1 depletion results in significant inhibition of cell viability of A549 and H358 cells (Fig. 2b). Colony formation assay indicated that MESP1 knockdown also significantly affects the growth ability of A549 and H358 cells as the number of colonies formed in knockdown cells were significantly lower (Fig. 2c). Transient overexpression of wildtype *MESP1*, but not a mutant that negatively affects DNA binding (E91A/K92A, hereafter EK-mutant), induced proliferation and clonal growth of A549 cells (Fig. 2d–f). Taken together, these results suggest that NSCLC cells are addicted to elevated expression of MESP1 and forced downregulation of MESP1 correlates with decrease in cell proliferation and growth advantage.

3.3. MESP1 cooperates with loss of ARF to induce cellular transformation

We next introduced FLAG-tagged wildtype or EK-mutant *MESP1* gene into immortalized normal human bronchial epithelial cells (BEAS-2B). Unexpectedly, the cells stably expressing wildtype MESP1 grew slower than the cells expressing the control vector or EK-mutant (Supplementary Fig. S2). This led us to examining the endogenous levels of tumor suppressor genes such as *p53, ARF*, which might be elevated in response to uncontrolled proliferation resulting from expression of an oncogene, as previously known in literature as "oncogenic stress" [23,24]. Interestingly, we found that levels of ARF were elevated in response to wildtype MESP1 protein expression but not the EK-mutant (Supplementary Fig. S2a). Complete absence of *ARF* expression is reported in 33% of lung squamous cell carcinoma cases [25] while *ARF* regulated pathway accounts for 15% of significantly mutated pathways in lung adenocarcinoma [26]. In response to expression of driver oncogenes such as *c-MYC*, ARF acts as an oncogenic sensor sequestering MDM2 in the nucleolus to stabilize p53 to trigger cell senescence [27]. Apart from p53 dependent functions, ARF induces cell senescence in a p53-independent way via interaction with proteins such as TIP60, HIF1a, ATM, and ATR among others [23]. Elevated levels of ARF and slow growth of MESP1 overexpressing cells (Supplementary Fig. S2) led us to hypothesize that absence of *ARF* is the oncogenic cooperation that *MESP1* needs to bring about oncogenic transformation. To test this hypothesis, we chose to overexpress *MESP1* in cells that have genetic deletion of ARF (ARF-/-) followed by assessment of proliferation, transformation and transcriptome analyses (Figs. 3–5).

We introduced doxycycline-inducible V5-tagged wildtype (wt) or EK-mutant Mesp1 (E85A/K86A) in p19ARF-/- mouse embryonic fibroblasts (MEFs) (Fig. 3a). Analysis at both RNA and protein level confirmed overexpression of Mesp1 in wildtype and EK-mutant Mesp1-transduced ARF -/- MEFs as compared to control (Fig. 3a). The growth rate of wt-Mesp1 ARF -/- MEFs was significantly higher than that of EK-mutant-Mesp1 or control ARF -/- MEFs (Fig. 3b). Consistent with this, wt-Mesp1 ARF -/- MEFs generated significantly more colonies as compared to EK-mutant-Mesp1 or control ARF -/- MEFs (Fig. 3c) in a colony formation assay, suggesting that Mesp1 overexpression results in growth advantage in these cells. As a measure of cellular transformation, we performed soft agar colony formation assay, and observed that wt-Mesp1 ARF -/- MEFs formed more colonies than control ARF -/- MEFs, whereas EK-mutant-Mesp1 ARF -/- MEFs failed to form any colonies on soft agar (Fig. 3d). On the other hand, Mesp1-overexpression did not induce survival, proliferation or transformation in MEFs null for *p53*, which still express ARF (Supplementary Fig. S3), suggesting that the loss of ARF but not p53 is essential for MESP1-mediated transformation. These data suggest that MESP1 expression causes 'oncogenic stress' in the presence of ARF and when ARF is absent, MESP1 expression results in increased cell proliferation, survival and transformation.

3.4. MESP1-driven gene signature is associated with multiple hallmarks of cancer

Our results suggest that MESP1 is required for proliferation of cancer cells, and induces transformation of primary cells. Mutations within the DNA-binding domain of Mesp1 failed to reproduce the phenotypic effects of wildtype Mesp1, which suggests that MESP1 may have essential transcription roles in these cell types. In order to determine genome-wide downstream transcriptional targets of MESP1, we performed RNA-Seq in ARF-/- MEFs expressing wt- or EK-mutant Mesp1, and compared these datasets to gene expression profiles obtained in MESP1-depleted A549 cell lines (Fig. 4). We first determined differentially expressed genes (DEGs) by comparing wt- vs. EK-mutant Mesp1 ARF-/- MEFs and obtained 1100 genes whose

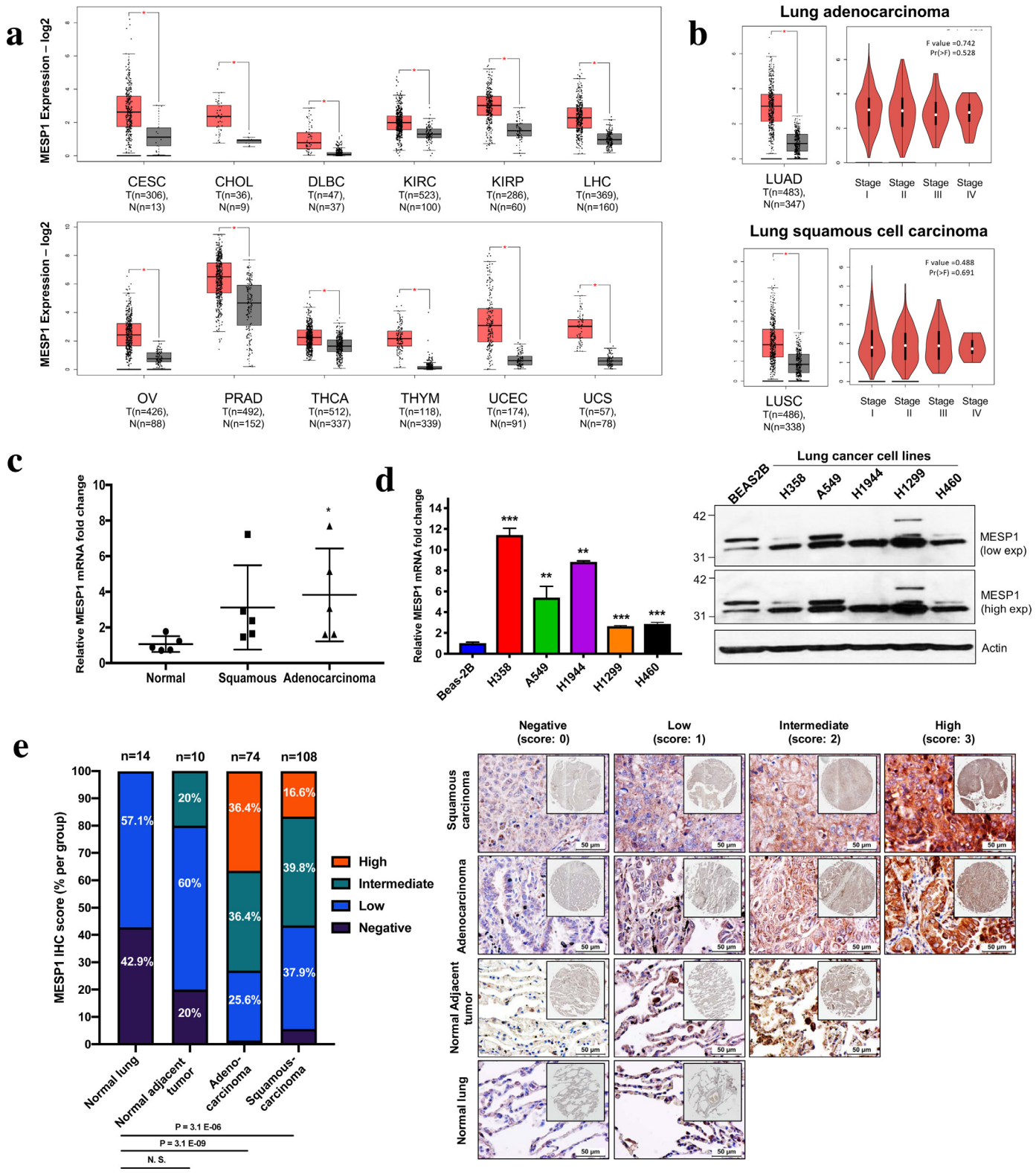

Fig. 1. MESP1 expression is associated with non-small cell lung cancer. (a) MESP1 transcript expression in various normal (grey colored) versus cancerous patients (orange colored) and (b) MESP1 transcript expression in normal versus lung adenocarcinoma patients (various stages) (top); MESP1 expression in normal and lung squamous cell carcinoma patients (various stages) (bottom), from TCGA and GTEx datasets. (c) qRT-PCR analysis of MESP1 mRNA in RNA samples from normal lung, lung squamous cell carcinoma and lung adenocarcinoma patients. (d) qRT-PCR analysis of MESP1 mRNA and immunoblots (low and high exposure) of MESP1 to check for endogenous level of hMESP1 in Beas-2B, H358, A549, H1944, H1299 and H460 cell lines. β–ACTIN was used as the housekeeping gene for normalization in qRT-PCR analysis and also as a loading control for western blot. The upper band in MESP1 immunoblot represents a likely modification. (e) Representative images at 5X and 40X magnification (right) of MESP1-immunohistochemical (IHC) staining from lung tissue arrays, including tissues from normal lung, normal adjacent tumor, lung adenocarcinoma, and lung squamous cell carcinoma. IHC scores are determined by staining intensity and percentage of stained cells; (left) quantification according to cytoplasmic IHC expression of MESP1 in tumor specimens including normal lung and normal adjacent tumor tissues. In all panels, data are represented as mean ± SD. * $p < 0.05$; ** $p < 0.01$; *** $p < 0.001$ (by two-tailed Student's *t*-test). (For interpretation of the references to color in this figure legend, the reader is referred to the web version of this article).

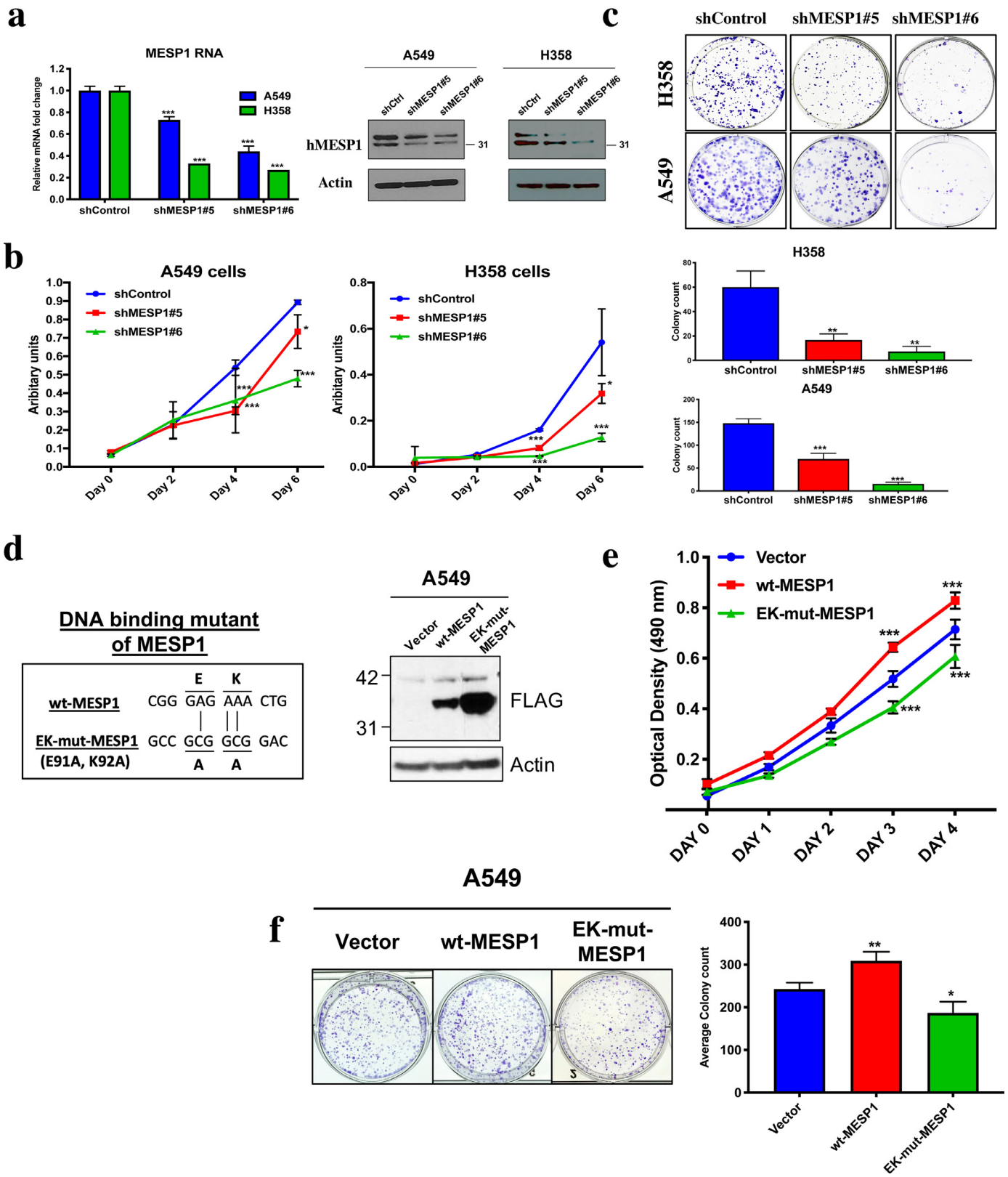

Fig. 2. MESP1 regulates growth and cell proliferation of NSCLC cells. (a) qRT-PCR and immunoblot of hMESP1 in shControl, shMESP1#5 and shMESP1#6 in A549 and H358 cells. β-Actin serves as the loading control. (b) Cell proliferation analysis by MTS assay of shControl, shMESP1#5 and shMESP1#6 in A549 and H358 cell lines. (c) Colony formation assay of shControl, shMESP1#5 and shMESP1#6 in A549 and H358 cells and quantification of colonies per well ± SD (bottom). (d) Schematic representation of the DNA-binding mutant of MESP1, with amino-acid residues responsible for DNA-binding shown by vertical lines (left), and immunoblot (right) of A549 cells transiently expressing MESP1 (FLAG-tagged) for control, wt-MESP1 and EK-mutant-MESP1. (e) Cell proliferation analysis by MTS. (f) Colony formation assay of control, wt-MESP1 and EK-mutant-MESP1 A549 cells (left) with quantification of colonies per field (right). In all panels, data are represented as mean ± SD. * $p < 0.05$; ** $p < 0.01$; *** $p < 0.001$ (by two-tailed Student's *t*-test).

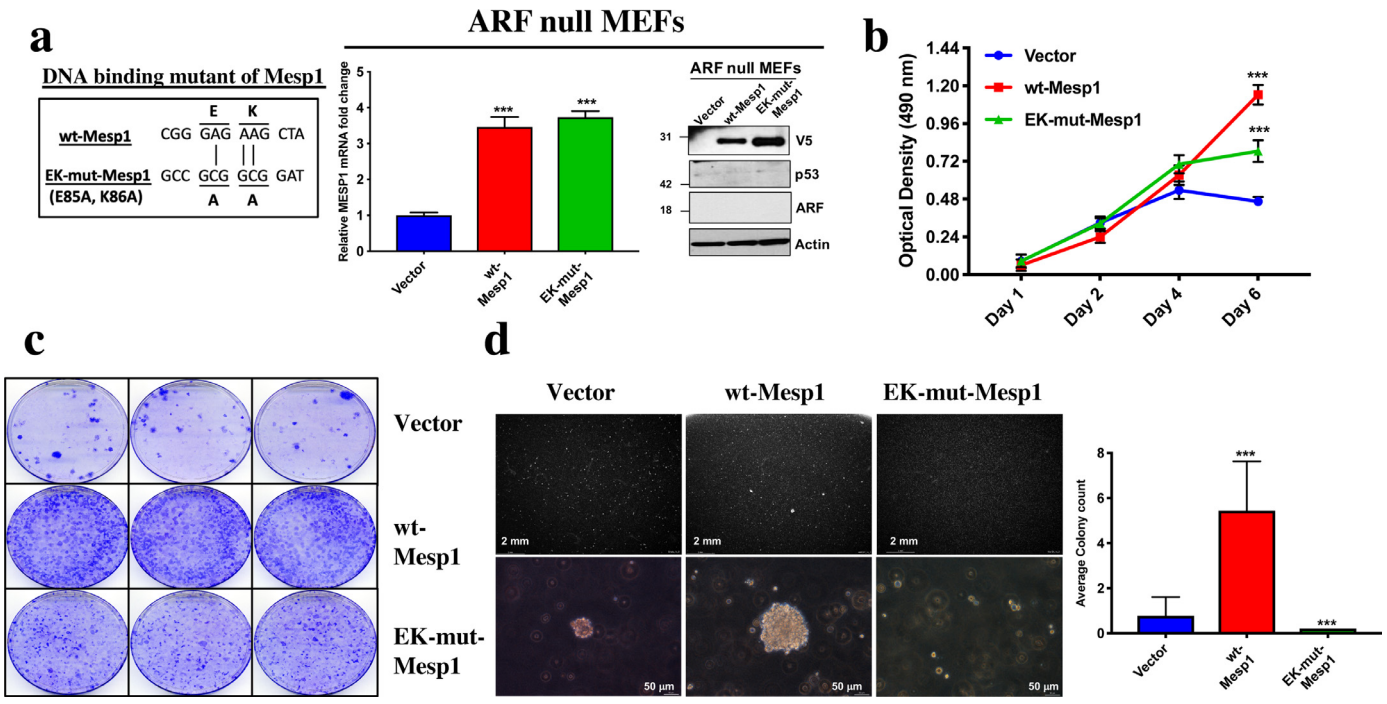

Fig. 3. MESP1 causes oncogenic transformation of ARF null MEFs. (a) Schematic representation of the DNA-binding mutant of Mesp1, with amino-acid residues responsible for DNA-binding shown by vertical lines (left); qRT-PCR and immunoblot (right) of Mesp1 (V5-tag) for control, wt-Mesp1 and EK-mutant-Mesp1 ARF -/- MEFs. (b and c) Cell proliferation analysis by MTS (b) and colony formation assay (c) of control, wt-Mesp1 and EK-mutant-Mesp1 ARF -/- MEFs. (d) Anchorage-independent growth of control, wt-Mesp1 and EK-mutant-Mesp1 ARF -/- MEFs as determined using a soft agar colony formation assay. Representative images of colonies in soft agar (left) and quantification of the colonies per field (right). Scale bar: 2 mm (low magnification) and 50 µm (higher magnification). In all panels, data are represented as mean ± SD. * $p < 0.05$; ** $p < 0.01$; *** $p < 0.001$ (by two-tailed Student's *t*-test).

expression is dependent on wt- Mesp1 (Fig. 4a). Next, we determined MESP1-dependent DEGs in A549 cells (Fig. 4b), and overlapped these genes to the DEGs contingent upon wt-Mesp1 overexpression, to identify potential transcriptional targets of MESP1 (Fig. 4c).

For ARF -/- MEFs, 1100 genes were found to be differentially expressed in wt-Mesp1 cells when compared to control and EK-mutant Mesp1 cells. 399 genes were upregulated, whereas 701 genes were downregulated (Fig. 4a). On the other hand, upon MESP1-knockdown, 1118 genes showed differential expression when compared to control: 706 genes were downregulated, while 412 genes were upregulated (Fig. 4b). For a complete list of differentially regulated genes, see Supplementary Table T4.

We next intersected Mesp1-overexpressing (MESP1-OE) and MESP1-knockdown (MESP1-KD) DEGs to find overlapping genes (Fig. 4c). 91 genes were found to be common between the two sets (Fig. 4c and d). To test for enriched hallmarks of cancer, GSEA mSigDB analysis of MESP1-OE DEGs, MESP-KD DEGs, as well as of the 91 common genes was performed. Interestingly, all 3 lists individually showed enrichment for similar hallmarks of cancer. EMT was the most significantly enriched, along-with other hallmarks such as Hypoxia, TNFα signaling, Glycolysis and Estrogen response (Fig. 4d).

In order to determine direct targets of MESP1, we next intersected upregulated genes of MESP1-overexpressing DEGs with downregulated genes of MESP1-knockdown DEGs (Fig. 5a). 24 genes were found to be putative direct targets of MESP1, majority of which have established functions in cancer disease initiation and progression. To test if MESP1 directly regulates their expression, we first performed qRT-PCR to examine the relative levels of their mRNA transcripts in MESP1 knockdown A549 and H358 cancer cell lines. The gene signature was validated because MESP1-KD cells showed decreased expression of Insulin like growth factor binding protein-4 (*IGFBP4*), Serpin Family B member 9 (*SERPBINB9*), Connective tissue growth factor (*CTGF*), Tensin 1 (*TNS1*), Muscle Ras Oncogene Homolog (*MRAS*), Mesoderm specific transcript (*MEST*), Ras homolog family member U (*RHOU*) and Fms related tyrosine kinase 4 (*FLT4*) (Fig. 5b and c). Next, to test if MESP1 overexpression activates the expression of these genes and if the DNA-binding function of MESP1 is critical for this regulation, we measured the expression of these genes by qRT-PCR in wt and EK-mutant Mesp1 expressing cells. As expected, expression of *Igfbp4, Serpinb9, Ctgf, Tns1, Mras, Mest, Rhou* and *Flt4* was significantly induced in wt-Mesp1 overexpressing cells compared to control cells. On the other hand, the expression of MESP1-targets was significantly reduced in cells expressing EK-mutant-Mesp1 as compared to wt-Mesp1 (Fig. 5d). This suggests that the expression of these genes is dependent on DNA-binding ability of MESP1. Besides these, 19 genes were upregulated in MESP1-KD cells and downregulated on MESP1-OE cells. By qRT-PCR analysis, expression of one gene from this list, *EMP3,* was verified (Fig. 5b–d). *EMP3*, a known tumor suppressor in gliomas, neuroblastomas and esophageal squamous cell carcinoma [28,29], appears to be suppressed by MESP1.

Next, we performed ChIP-qPCR analyses to further confirm that expression of target genes is dependent on direct recruitment of MESP1 at their loci. MESP1 is a bHLH transcription factor that preferably binds to DNA regions containing E-box binding motif [11]. We searched the ChIP-seq datasets of E-box binding factors such as MYC, MAX, USF1, USF2, TAL1 and TCF12 available through ENCODE consortium [30–32] and identified E-box binding motifs within the genomic locus of MESP1-target genes (Supplementary Fig. S5). Oligonucleotides were designed encompassing these motifs and enrichment of MESP1 was tested by ChIP-qPCR. Our results show that MESP1 was enriched to the chromatin loci of all the genes tested as compared to IgG control. Therefore, *IGFBP4, FLT4, MRAS, CTGF, MEST* and *EMP3* are likely direct targets of MESP1 (Fig. 5e).

To determine the prognostic value of MESP1 along with MESP1-regulated 24-gene signature, Kaplan-Meier survival analysis was performed. In lung squamous cell carcinoma (LUSC) dataset, MESP1-regulated 24 genes were significantly correlated with poor survival [Logrank $p = 0.015$, Hazard ratio (HR)=1.5] (Supplementary Fig. S4a).

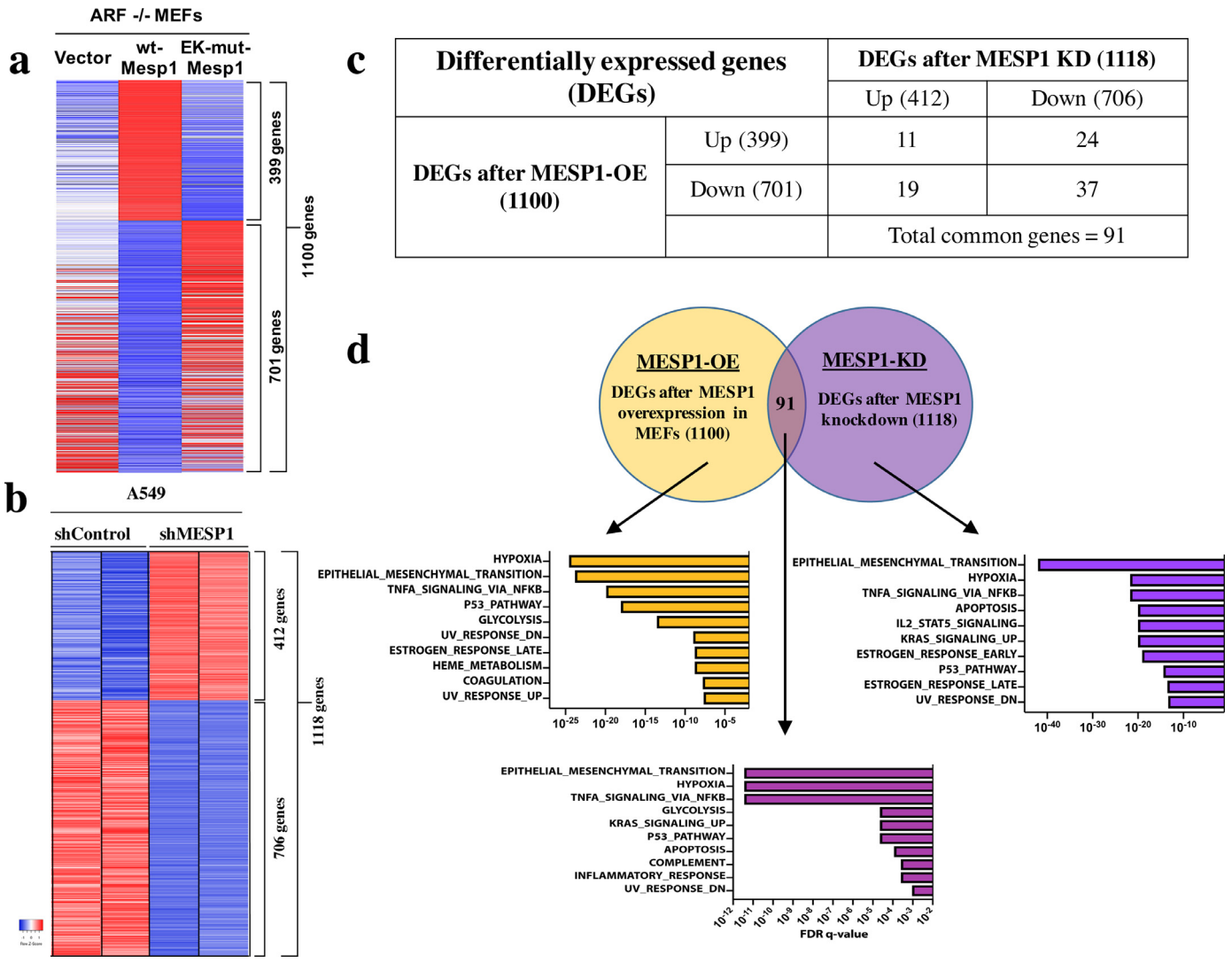

Fig. 4. MESP1 dependent genes encompass various hallmarks of cancer. (a) Heat map of differentially regulated genes (DEGs) in control, wt-Mesp1 and EK-mutant-Mesp1 $p19^{ARF}$ -/- MEFs. (b) Heat map of differentially regulated genes in shControl and shMESP1#6 expressing A549 cells. (c and d) Table (c) and Venn diagram (d) showing an overall overlap between DEGs upon Mesp1-overexpression (MESP1-OE) in ARF -/- MEFs and MESP1-knockdown (MESP1-KD) in A549 cells and bar graphs for mSigDB-GSEA hallmark analysis of respective gene lists (Bottom).

Intriguingly, the survival curve further worsens with addition of MESP1 to the 24-gene list [Logrank $p = 0.00066$, Hazard ratio (HR) = 1.8] (Fig. 5f). However, significant correlation could not be established for LUAD dataset. Taken together, these results suggest that MESP1 directly regulates the expression of a gene signature, which is important in multiple hallmarks of cancer and correlates with poor patient survival.

3.5. Suppression of MESP1 inhibits tumor growth in xenograft animal model

To validate our in vitro findings and to evaluate the effect of MESP1 knockdown in tumor growth in vivo, xenograft assays were performed. To this end, immunodeficient NSG mice were subcutaneously injected with lung cancer cells (H358 and A549) stably transduced with shMESP1(#5 or #6) and shControl hairpins. Tumors of shMESP1 treated groups weighed lighter as compared to the control group as shown in Fig. 6a (A549 cells) and Fig. 6e (H358 cells). Tumor volume for shMESP1 treated A549 cells and H358 cells (Fig. 6b and Supplementary Fig. S4c, respectively) was significantly lower than the control group. For A549 cells, mice were sacrificed 38 days post-injection whereas for H358 cells, mice were sacrificed 15 days post-injection and tumors were resected respectively (Fig. 6c and Supplementary Fig. S4b). H&E staining of both A549 (Fig. 6d) and H358 (Fig. 6f) tumors revealed more aggressive invasion into the surrounding tissues at the periphery for shControl tumors as compared with both shMESP1#5 and shMESP1#6 tumors. For detailed histopathology report, see Supplementary Table T5.

4. Discussion

Lung cancer is the second most commonly diagnosed cancer and the leading cause of cancer deaths in the United States [1,2]. Although there has been a remarkable progress in understanding the molecular mechanisms that drive lung cancer progression, there still exists the need of better understanding of tumor dependencies encompassing lineage addiction models. In this study, we report for the first time that MESP1, a master regulator of embryonic development, is highly expressed in lung cancer and functions as a lineage-survival oncogene. MESP1 plays an essential role in mesoderm derived cardiovascular lineage development [11]. MESP1-regulated transcriptomic analyses in differentiating embryoid bodies showed upregulation of gene targets involved in mesoderm as well as endoderm lineage, pertaining to lung development [10]. In this context, the master regulatory role of MESP1

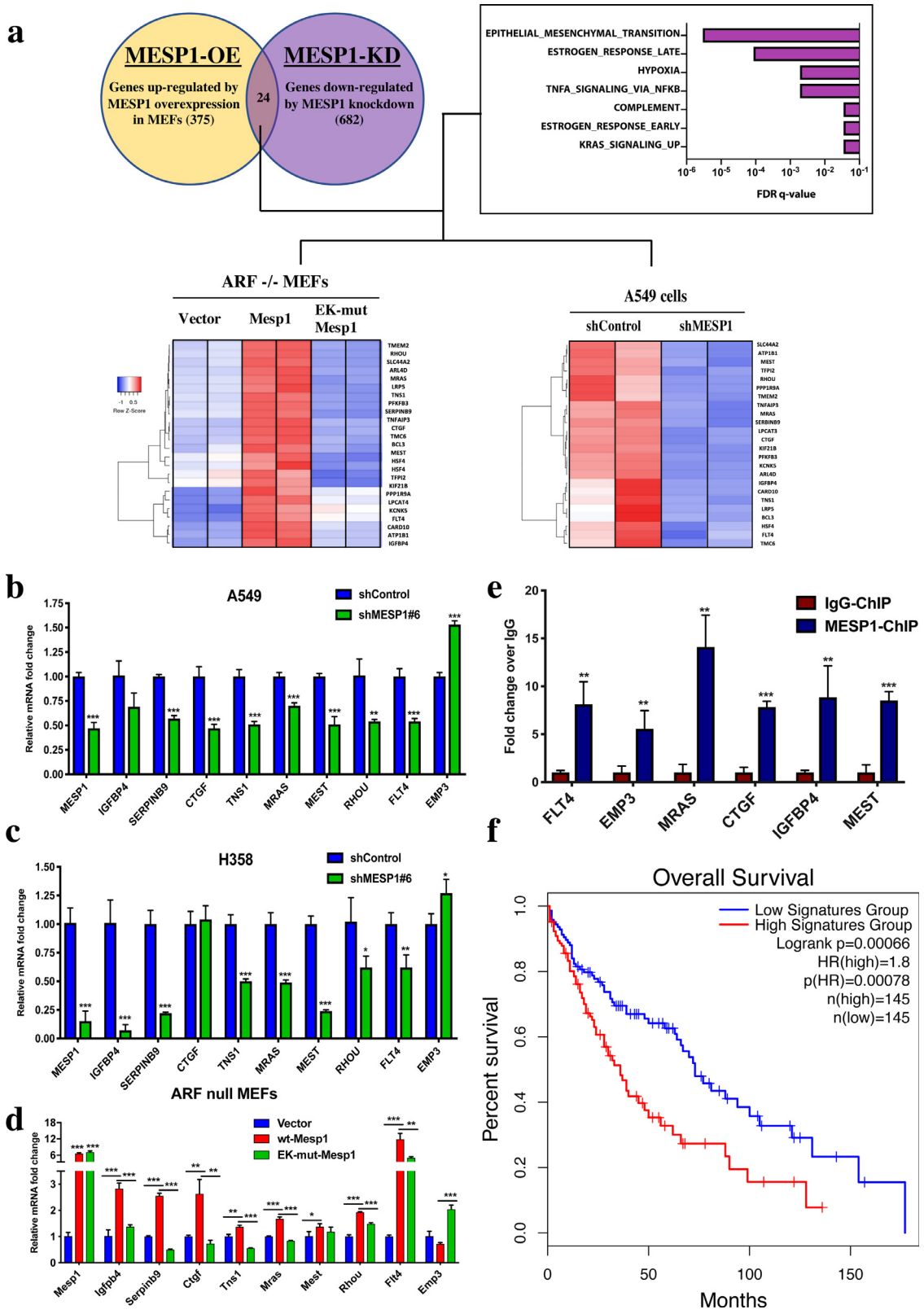

Fig. 5. Identification of 24 MESP1 target genes that predict poor prognosis. (a) Venn diagram (left) and bar graph for mSigDB-GSEA hallmark analysis (right) of overlapping genes across genes upregulated by Mesp1 overexpression in ARF -/- MEFs and genes-downregulated by MESP1-knockdown in A549 cells; and heat map of overlapping genes in corresponding systems (bottom). (b, c and d) qRT-PCR analysis of corresponding genes upon MESP1 knockdown in A549 (b) and H358 (c) cells and upon Mesp1-overexpression (d) in ARF -/- MEFs. (e) ChIP assay of endogenous MESP1 for target genes, presented as fold enrichment for MESP1 antibody over IgG antibody control in H358 cells. (f) Kaplan–Meier Curve for overall survival of LUSC patients segregated by low or high expression of the 24 gene signature together with MESP1. In all panels, data are represented as mean ± SD. * $p < 0.05$; ** $p < 0.01$; *** $p < 0.001$ (by two-tailed Student's *t*-test).

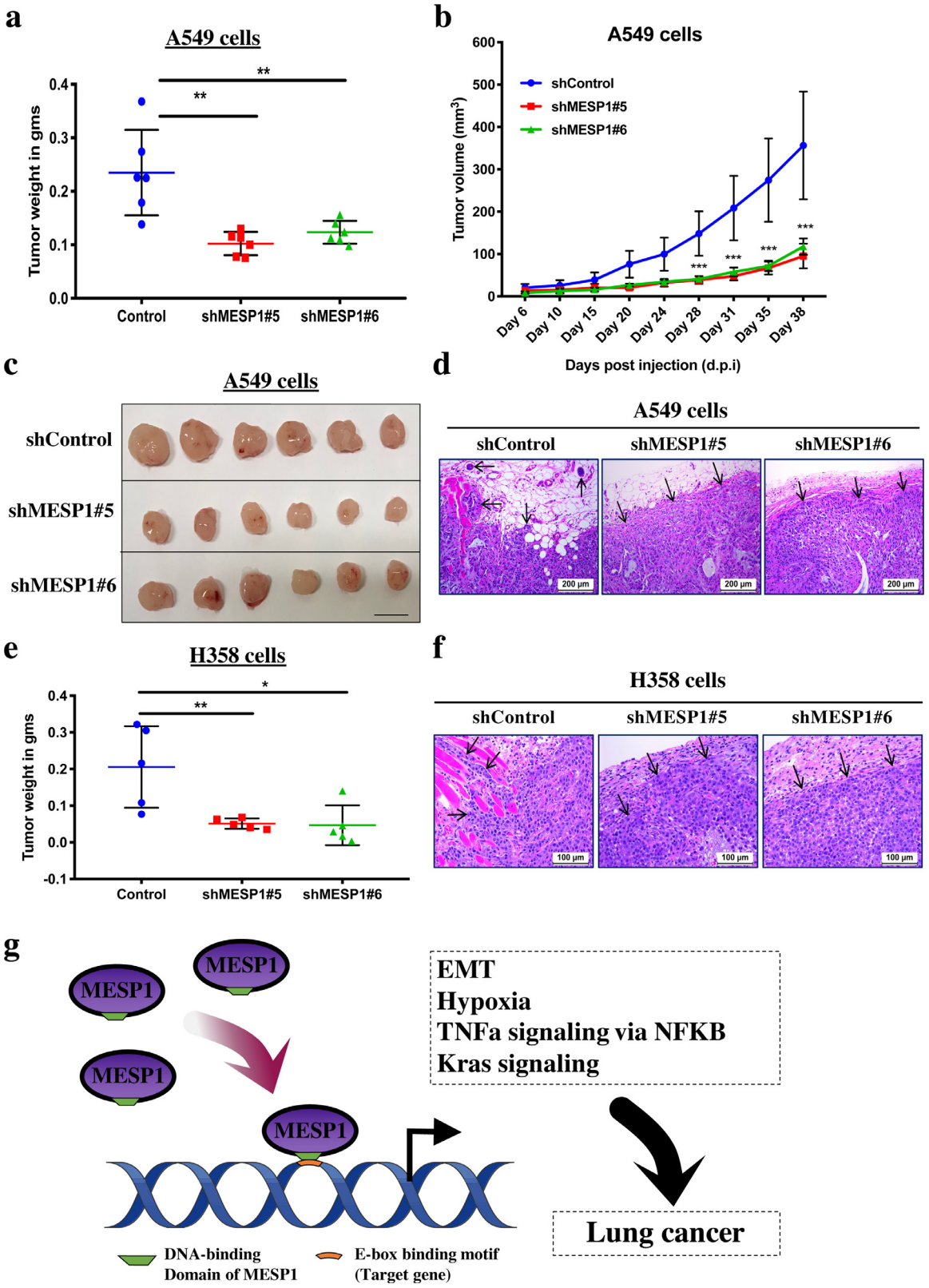

Fig. 6. MESP1 knockdown cells have reduced tumor formation. (a, b and c) Tumor weight (a), tumor volume (b) and tumor images (c) after 38 days post subcutaneous injection of shControl, shMESP1#5 and shMESP1#6 stably transduced A549 cells in NSG mice. (d) H&E staining of tumors obtained from NSG mice injected with shControl, shMESP1#5 and shMESP1#6 stably transduced A549 cells. (e and f) Tumor weight (e) and H&E staining (f) of tumors obtained from NSG mice after 15 days post subcutaneous injection of shControl, shMESP1#5 and shMESP1#6 stably transduced H358 cells. (g) Schematic representation of MESP1's function as a lineage-survival oncogene in lung cancer. In all panels, data are represented as mean ± SD. * $p < 0.05$; ** $p < 0.01$; *** $p < 0.001$ (by two-tailed Student's *t*-test).

in cell-survival mechanisms of developing heart and lung befits the idea of MESP1 being a potential "lineage-survival" oncogene in tumors of mesoderm and endoderm (mesendoderm) origin. Recent studies indicate an increased interest in delineating lineage-based tumor survival and dependencies. For example, amplification of master melanocyte lineage regulator *MITF* in melanoma [6], amplification of normal lung development transcription factor *TITF-1* in adenocarcinoma [8], pulmonary neuroendocrine (NE) cell development transcription factor *ASCL1* in survival of NE-lung cancers [33] and amplification of intestinal lineage development transcription factor *CDX2* in colorectal cancer [34]. *MITF* and *ASCL1* are examples of lineage-survival oncogenes belonging to the same family of basic helix-loop-helix (b-HLH) transcription factors as MESP1 [35].

Our profiling of available cancer genome [20–22] data reveal that MESP1 is overexpressed across all stages of lung adenocarcinoma and squamous cell carcinoma. To determine the functional significance of MESP1, we used two shRNAs targeting MESP1 by varying degrees in NSCLC-derived cells and observed that proliferation of these cells depend on MESP1 in a dose-dependent manner. We utilize MEFs depleted of $p19^{ARF}$ to examine MESP1 oncogenic cooperation. $p14^{ARF}$ ($p19^{ARF}$ in mouse) is a well-established tumor suppressor whose expression is robustly reduced across various cancers [36,37]. We showed that MESP1 was able to transform mouse embryonic fibroblasts in p19ARF-null background but not p53-null background. These interesting observations suggest that MESP1 cooperates with the loss of tumor suppressor p19ARF to achieve oncogenesis. In fact, many proteins require oncogenic cooperation to transform immortalized cells, such as between *SOX2* and *FGFR2* or *FOXE1*[7], between *MITF* and mutant $BRAF^{V600E}$[6] and between *TTF1/NKX2-1*, *NKX2-8* and *PAX9* [38]. To delineate the genetic background(s) that are more suitable for MESP1 mediated oncogenic transformation will be an exciting area of further investigations.

Our genome-wide transcriptome analyses revealed several putative direct targets of MESP1 that play essential roles in cancer, suggesting MESP1 is an important transcription factor in lung tumorigenesis. To reveal the direct targets of transcription factor MESP1 and to determine MESP1-regulated putative transcriptome, we used the strategy of employing a DNA-binding mutant version of MESP1. To this end, we generated MEFs stably expressing wildtype or DNA-binding mutant Mesp1 in p19ARF-/- background and performed RNA-Seq to identify DEGs that are most likely dependent on DNA-binding ability of Mesp1. In parallel, we depleted MESP1 from NSCLC-derived cancer cells and also determined MESP1-dependent genes. Comparative analyses of likely MESP1-targets (DEGs from wt vs. EK-mutant Mesp1 MEFs) and MESP1-dependent genes (DEGs from MESP1-depleted NSCLCs) resulted in a gene signature of 24 genes, as putative direct targets of MESP1 in lung cancer. These include several genes with essential roles in cancer such as, *SERPINB9/PI-9* that inhibits granzyme B, which is required for cytotoxic lymphocyte mediated killing of tumor cells, thus felicitating immune escape by tumors [39]; *MRAS*, which as a part of a ternary complex, promotes oncogenic transformation by activating ERK pathway [40]. Interestingly, our gene set enrichment analyses of the MESP1 targets revealed that majority of the genes have noted roles in cancer progression, especially EMT; such as, *IGFBP4* promotes invasion and metastasis in renal cell carcinoma and glioblastoma by regulating key factors of EMT and tumor progression [41,42], *CTGF* expression is critical for migration and invasion of breast cancer and melanoma cells [43,44], loss of imprinting of MEST promotes invasiveness of breast cancer cells [45], FLT-4 with its ligand VEGF-C promotes metastasis and invasion of lung adenocarcinoma cells via its target contactin-1 [46]. Involvement of MESP1 and its targets in EMT found here is reminiscent of the well-established role of MESP1 in EMT during normal development [14–16], and remains an exciting area for further investigations. Moreover, the mechanisms that result in aberrant expression of MESP1 in lung cancer remain unknown. Several upstream regulators of MESP1 such as Brachyury (T), Eomes and Tbx6 have been reported previously [47]; how these integrate MESP1 expression with lung cancer progression and pathogenesis will be investigated in the future.

Taken together, we demonstrate that upregulation of MESP1, a key tumor-promoting alteration, functions to create tumor dependency on an inbuilt lineage-survival process. MESP1, being the nodal point of this survival process, sustains the tumor dependency by transcriptionally activating key genes involved in tumor cell initiation, proliferation and progression including EMT (Fig. 6g). In conclusion, our findings for the first time indicate an important role for MESP1 in cancer and as a novel biomarker in NSCLC, making it a potential therapeutic target for the disease.

Declaration of competing interest

The authors declare no competing financial interests.

CRediT authorship contribution statement

Neha Tandon: Formal analysis, Investigation, Writing - original draft, Writing - review & editing. **Kristina Goller:** Investigation, Methodology. **Fan Wang:** Investigation, Methodology. **Benjamin Soibam:** Investigation, Methodology. **Mihai Gagea:** Writing - review & editing. **Abhinav K. Jain:** Writing - review & editing. **Robert J. Schwartz:** Writing - review & editing. **Yu Liu:** Formal analysis, Funding acquisition, Project administration, Supervision, Writing - review & editing.

Acknowledgments

We are thankful to Dr. Michelle C. Barton and Dr. Daniel E. Frigo at The University of Texas MD Anderson Cancer Center for helpful discussions. We thank Dr. Martine F. Roussel at St. Jude Children's Research Hospital for providing cell lines and plasmids. We thank Dr. M. David Stewart, Dr. Dinakar Iyer, and other members of Liu laboratory and Schwartz laboratory for help during the course of the project.

Funding sources

This research is supported by a faculty startup grant from University of Houston, a grant from Congressionally Directed Medical Research Programs (LC140601), and a grant from Elsa U. Pardee Foundation.

Data sharing statement

Transcriptome data generated in this study will be immediately available to the academic community upon publication of this manuscript. Request should be addressed to Yu Liu, Email: yliu54@uh.edu.

Supplementary materials

Supplementary material associated with this article can be found in the online version at doi:10.1016/j.ebiom.2019.11.012.

References

[1] Ferlay J, Soerjomataram I, Dikshit R, Eser S, Mathers C, Rebelo M, et al. Cancer incidence and mortality worldwide: sources, methods and major patterns in GLOBOCAN 2012. Int J Cancer 2015;136(5):E359–86.
[2] Siegel RL, Miller KD, Jemal A. Cancer statistics, 2018. CA Cancer J Clin 2018;68(1):7–30.
[3] Chen Z, Fillmore CM, Hammerman PS, Kim CF, Wong KK. Non-small-cell lung cancers: a heterogeneous set of diseases. Nat Rev Cancer 2014;14(8):535–46.
[4] Howlader N, Noone AM, Krapcho M, Miller D, Brest A, Yu M, Ruhl J, Tatalovich Z, Mariotto A, Lewis DR, Chen HS, Feuer EJ, Cronin KA (eds). SEER Cancer Statistics Review, 1975-2016, National Cancer Institute. Bethesda, MD, https://seer.cancer.gov/csr/1975_2016/, based on November 2018 SEER data submission, posted to the SEER web site, April 2019.
[5] Garraway LA, Sellers WR. Lineage dependency and lineage-survival oncogenes in human cancer. Nat Rev Cancer 2006;6(8):593–602.

[6] Garraway LA, Widlund HR, Rubin MA, Getz G, Berger AJ, Ramaswamy S, et al. Integrative genomic analyses identify MITF as a lineage survival oncogene amplified in malignant melanoma. Nature 2005;436(7047):117–22.
[7] Bass AJ, Watanabe H, Mermel CH, Yu S, Perner S, Verhaak RG, et al. SOX2 is an amplified lineage-survival oncogene in lung and esophageal squamous cell carcinomas. Nat Genet 2009;41(11):1238–42.
[8] Kwei KA, Kim YH, Girard L, Kao J, Pacyna-Gengelbach M, Salari K, et al. Genomic profiling identifies TITF1 as a lineage-specific oncogene amplified in lung cancer. Oncogene 2008;27(25):3635–40.
[9] Liang Q, Xu C, Chen X, Li X, Lu C, Zhou P, et al. The roles of MESP family proteins: functional diversity and redundancy in differentiation of pluripotent stem cells and mammalian mesodermal development. Protein Cell 2015;6(8):553–61.
[10] Soibam B, Benham A, Kim J, Weng KC, Yang L, Xu X, et al. Genome-Wide identification of MESP1 targets demonstrates primary regulation over mesendoderm gene activity. Stem Cells 2015;33(11):3254–65.
[11] Bondue A, Blanpain C. Mesp1: a key regulator of cardiovascular lineage commitment. Circ Res 2010;107(12):1414–27.
[12] Islas JF, Liu Y, Weng KC, Robertson MJ, Zhang S, Prejusa A, et al. Transcription factors ETS2 and MESP1 transdifferentiate human dermal fibroblasts into cardiac progenitors. Proc Natl Acad Sci U S A 2012;109(32):13016–21.
[13] Chan SS, Shi X, Toyama A, Arpke RW, Dandapat A, Iacovino M, et al. Mesp1 patterns mesoderm into cardiac, hematopoietic, or skeletal myogenic progenitors in a context-dependent manner. Cell Stem Cell 2013;12(5):587–601.
[14] Eskildsen TV, Ayoubi S, Thomassen M, Burton M, Mandegar MA, Conklin BR, et al. MESP1 knock-down in human iPSC attenuates early vascular progenitor cell differentiation after completed primitive streak specification. Dev Biol 2019;445(1):1–7.
[15] Chiapparo G, Lin X, Lescroart F, Chabab S, Paulissen C, Pitisci L, et al. Mesp1 controls the speed, polarity, and directionality of cardiovascular progenitor migration. J Cell Biol 2016;213(4):463–77.
[16] Lescroart F, Wang X, Lin X, Swedlund B, Gargouri S, Sanchez-Danes A, et al. Defining the earliest step of cardiovascular lineage segregation by single-cell RNA-seq. Science 2018;359(6380):1177–81.
[17] Tandon N, Thakkar KN, LaGory EL, Liu Y, Giaccia AJ. Generation of stable expression mammalian cell lines using lentivirus. Bio Protoc 2018;8(21):e3073.
[18] Pathiraja TN, Thakkar KN, Jiang S, Stratton S, Liu Z, Gagea M, et al. TRIM24 links glucose metabolism with transformation of human mammary epithelial cells. Oncogene 2015;34(22):2836–45.
[19] Liberzon A, Subramanian A, Pinchback R, Thorvaldsdottir H, Tamayo P, Mesirov JP. Molecular signatures database (MSigDB) 3.0. Bioinformatics 2011;27(12):1739–40.
[20] Tang Z, Li C, Kang B, Gao G, Li C, Zhang Z. GEPIA: a web server for cancer and normal gene expression profiling and interactive analyses. Nucl Acids Res 2017;45(W1):W98–W102.
[21] Cerami E, Gao J, Dogrusoz U, Gross BE, Sumer SO, Aksoy BA, et al. The cBio cancer genomics portal: an open platform for exploring multidimensional cancer genomics data. Cancer Discov 2012;2(5):401–4.
[22] Gao J, Aksoy BA, Dogrusoz U, Dresdner G, Gross B, Sumer SO, et al. Integrative analysis of complex cancer genomics and clinical profiles using the cBioPortal. Sci Signal 2013;6(269):l1.
[23] Sherr CJ. Divorcing ARF and p53: an unsettled case. Nat Rev Cancer 2006;6(9):663–73.
[24] Matheu A, Maraver A, Serrano M. The ARF/p53 pathway in cancer and aging. Cancer Res 2008;68(15):6031–4.
[25] Cancer Genome Atlas Research N. Comprehensive genomic characterization of squamous cell lung cancers. Nature 2012;489(7417):519–25.
[26] Ding L, Getz G, Wheeler DA, Mardis ER, McLellan MD, Cibulskis K, et al. Somatic mutations affect key pathways in lung adenocarcinoma. Nature 2008;455(7216):1069–75.
[27] Sherr CJ, Weber JD. The ARF/p53 pathway. Curr Opin Genet Dev 2000;10(1):94–9.
[28] Alaminos M, Davalos V, Ropero S, Setien F, Paz MF, Herranz M, et al. EMP3, a myelin-related gene located in the critical 19q13.3 region, is epigenetically silenced and exhibits features of a candidate tumor suppressor in glioma and neuroblastoma. Cancer Res 2005;65(7):2565–71.
[29] Fumoto S, Hiyama K, Tanimoto K, Noguchi T, Hihara J, Hiyama E, et al. EMP3 as a tumor suppressor gene for esophageal squamous cell carcinoma. Cancer Lett 2009;274(1):25–32.
[30] Gerstein MB, Kundaje A, Hariharan M, Landt SG, Yan KK, Cheng C, et al. Architecture of the human regulatory network derived from ENCODE data. Nature 2012;489(7414):91–100.
[31] Wang J, Zhuang J, Iyer S, Lin X, Whitfield TW, Greven MC, et al. Sequence features and chromatin structure around the genomic regions bound by 119 human transcription factors. Genome Res 2012;22(9):1798–812.
[32] Wang J, Zhuang J, Iyer S, Lin XY, Greven MC, Kim BH, et al. Factorbook.org: a wiki-based database for transcription factor-binding data generated by the ENCODE consortium. Nucl Acids Res 2013;41(Database issue):D171–6.
[33] Augustyn A, Borromeo M, Wang T, Fujimoto J, Shao C, Dospoy PD, et al. ASCL1 is a lineage oncogene providing therapeutic targets for high-grade neuroendocrine lung cancers. Proc Natl Acad Sci U S A 2014;111(41):14788–93.
[34] Salari K, Spulak ME, Cuff J, Forster AD, Giacomini CP, Huang S, et al. CDX2 is an amplified lineage-survival oncogene in colorectal cancer. Proc Natl Acad Sci U S A 2012;109(46):E3196–205.
[35] Skinner MK, Rawls A, Wilson-Rawls J, Roalson EH. Basic helix-loop-helix transcription factor gene family phylogenetics and nomenclature. Differentiation 2010;80(1):1–8.
[36] Esteller M, Corn PG, Baylin SB, Herman JG. A gene hypermethylation profile of human cancer. Cancer Res 2001;61(8):3225–9.
[37] Ozenne P, Eymin B, Brambilla E, Gazzeri S. The ARF tumor suppressor: structure, functions and status in cancer. Int J Cancer 2010;127(10):2239–47.
[38] Kendall J, Liu Q, Bakleh A, Krasnitz A, Nguyen KC, Lakshmi B, et al. Oncogenic cooperation and coamplification of developmental transcription factor genes in lung cancer. Proc Natl Acad Sci U S A 2007;104(42):16663–8.
[39] Medema JP, de Jong J, Peltenburg LT, Verdegaal EM, Gorter A, Bres SA, et al. Blockade of the granzyme B/perforin pathway through overexpression of the serine protease inhibitor PI-9/SPI-6 constitutes a mechanism for immune escape by tumors. Proc Natl Acad Sci U S A 2001;98(20):11515–20.
[40] Young LC, Hartig N, Munoz-Alegre M, Oses-Prieto JA, Durdu S, Bender S, et al. An MRAS, SHOC2, and SCRIB complex coordinates ERK pathway activation with polarity and tumorigenic growth. Mol Cell 2013;52(5):679–92.
[41] Ueno K, Hirata H, Majid S, Tabatabai ZL, Hinoda Y, Dahiya R. IGFBP-4 activates the Wnt/beta-catenin signaling pathway and induces M-CAM expression in human renal cell carcinoma. Int J Cancer 2011;129(10):2360–9.
[42] Praveen Kumar VR, Sehgal P, Thota B, Patil S, Santosh V, Kondaiah P. Insulin like growth factor binding protein 4 promotes GBM progression and regulates key factors involved in EMT and invasion. J Neurooncol 2014;116(3):455–64.
[43] Braig S, Wallner S, Junglas B, Fuchshofer R, Bosserhoff AK. CTGF is overexpressed in malignant melanoma and promotes cell invasion and migration. Br J Cancer 2011;105(2):231–8.
[44] Zhu X, Zhong J, Zhao Z, Sheng J, Wang J, Liu J, et al. Epithelial derived CTGF promotes breast tumor progression via inducing EMT and collagen I fibers deposition. Oncotarget 2015;6(28):25320–38.
[45] Pedersen IS, Dervan PA, Broderick D, Harrison M, Miller N, Delany E, et al. Frequent loss of imprinting of PEG1/MEST in invasive breast cancer. Cancer Res 1999;59(21):5449–51.
[46] Su JL, Yang PC, Shih JY, Yang CY, Wei LH, Hsieh CY, et al. The VEGF-C/Flt-4 axis promotes invasion and metastasis of cancer cells. Cancer Cell 2006;9(3):209–23.
[47] Liu Y. Earlier and broader roles of mesp1 in cardiovascular development. Cell Mol Life Sci 2017;74(11):1969–83.